

Corrolazines: New Frontiers in High-Valent Metalloporphyrinoid Stability and Reactivity

DAVID P. GOLDBERG

The Department of Chemistry, Johns Hopkins University,
3400 North Charles Street, Baltimore, Maryland 21218

Received February 22, 2007

ABSTRACT

The activation of dioxygen and its analogues, such as hydrogen peroxide, by metalloporphyrins leads to the generation of high-valent metal–oxo species. This process is critically important to heme-catalyzed reactions, such as for cytochrome P450, and synthetic porphyrin-catalyzed oxidations. We have synthesized a new ring-contracted porphyrinoid system called a corrolazine that is designed to stabilize high oxidation states, including high-valent metal–oxo species. The corrolazine ligand stabilizes manganese(V) terminal oxo and terminal imido complexes for isolation, both of which are only transiently observed with normal porphyrin macrocycles. Examination of both oxygen atom transfer and hydrogen atom abstraction reactions for the Mn(V)–oxo complex has led to a number of mechanistic insights regarding these transformations. The activation of H₂O₂ to give the Mn(V)–oxo complex exhibits some dramatic and unexpected axial ligand effects that call into question the normal role of axial ligands in O–O bond cleavage pathways.

Introduction

Naturally occurring porphyrins are critically important cofactors in the biological processing of dioxygen and its congeners, such as in O₂ transport (hemoglobin), peroxide removal (peroxidases and catalases), oxygen reduction (cytochrome *c* oxidase), and oxidative catalysis (cytochrome P450¹). Man-made porphyrins and their analogues provide convenient systems for testing mechanistic hypotheses regarding these fundamental processes, and have been designed to reproduce these functions for practical applications. In particular, the activation of O₂ and H₂O₂ by various metalloporphyrins to give high-valent metal–oxo complexes has been of intense interest because of the relevance to heme enzymes and because of the potential usefulness of these reactions in catalytic oxidation chemistry.² Significant synthetic efforts have been directed at varying the peripheral substituents of the porphyrin ligand with the aim of tuning the properties at the metal center. Our group has taken a different approach; we have focused on modifying the basic porphyrinoid nucleus itself.

David P. Goldberg received his B.A. degree in chemistry from Williams College in 1989 and his Ph.D. in chemistry from the Massachusetts Institute of Technology in 1995. He continued his studies as a NIH Postdoctoral Fellow at Northwestern University before beginning his independent career at Johns Hopkins University in 1998, where he is currently an Associate Professor in the Chemistry Department. His research interests in bioinorganic chemistry include porphyrinoid synthesis and reactivity and the construction of synthetic analogues of metalloenzymes.

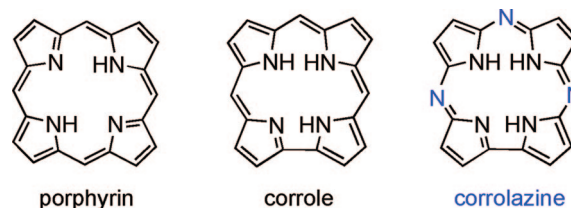


FIGURE 1. Core structures of porphyrin, corrole and corrolazine (Cz).

In 1998, we became interested in the ring-contracted porphyrinoid known as a corrole, which is missing one *meso* carbon atom (Figure 1). This molecule retains the tetrapyrrolic, aromatic structure of a porphyrin but is a 3– donor ligand when fully deprotonated. Our initial interest in these molecules stemmed from a few earlier reports that indicated corroles could stabilize high-valent oxidation states in transition metals,^{3–5} including a structurally characterized oxo-bridged diiron(IV) complex.⁶ From these papers, it seemed to us that corroles were ideal candidates for generating high-valent metal–oxo complexes and activating H₂O₂, O₂, and other biologically relevant oxidants. However, at this time, the syntheses of corroles were very laborious, and we set out to find a facile synthetic route for preparing a corrole-type ligand. We eventually targeted the *meso*-nitrogen-substituted analogues of corroles, which we now call “corrolazine” (Cz), because we recognized the possibility of an easy synthetic route involving a one-step “ring contraction”. This strategy proved to be correct, and we reported the successful synthesis of the first corrolazine in 2001.⁷ At about the same time, other groups reported facile syntheses for conventional corroles,^{8,9} and the field of corrole chemistry has since expanded enormously.

This Account will highlight recent advances in the chemistry of metallocorrolazines, emphasizing high-valent species and reactivity relevant to oxygen-derived processes in biology. An earlier review on corrolazines provides a broader perspective.¹⁰ We have shown that corrolazines are indeed capable of stabilizing high-valent oxidation states. A room-temperature-stable manganese(V)–oxo corrolazine complex was isolated, which can be generated from the activation of H₂O₂ under appropriate conditions. Mechanistic insights were obtained regarding oxygen atom transfer, hydrogen atom abstraction, and O–O bond cleavage reactions, all of which pertain to biologically relevant processes surrounding O₂ activation.

Corrolazine Synthesis

We were motivated to attempt the synthesis of the first corrolazine by reports of the direct conversion of phthalocyanine (Pc) to its ring-contracted corrole analogue, triazatetrazabenzcorrole (TBC).^{11–13} This one-step ring contraction was very attractive from a synthetic standpoint, and we speculated that the Pc starting material could be substituted with a tetraazaporphyrin precursor. Following the Pc methodology, the first corrolazine was prepared via the PBr₃-induced ring contraction of octakis(*tert*-

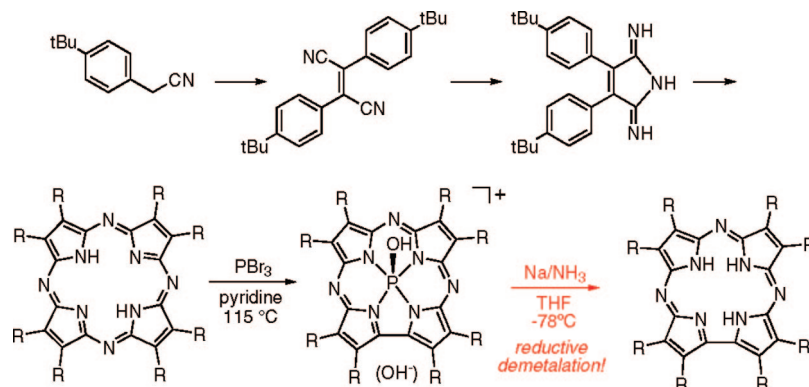


FIGURE 2. Synthesis of the first corrolazine, TBP_8CzH_3 .

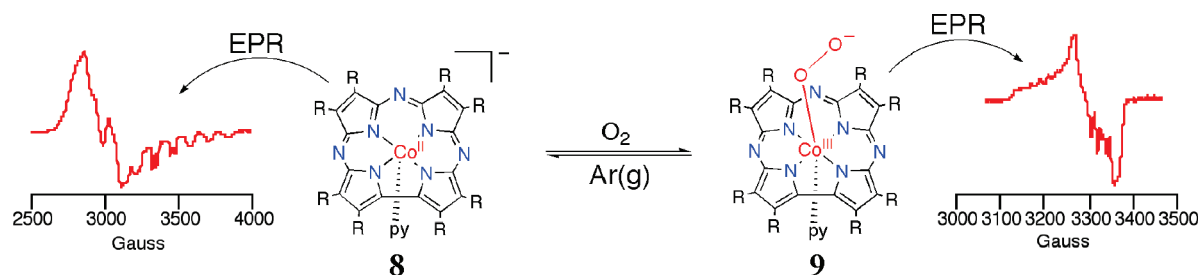


FIGURE 3. Reversible O_2 binding.

butylphenyl)-substituted tetraazaporphyrin (Figure 2), giving the phosphorus complex $[(\text{TBP}_8\text{Cz})\text{P}^{\text{V}}(\text{OH})]\text{OH}$ ($\text{TBP} = 4$ -*tert*-butylphenyl).⁷ Removing the phosphorus from the central cavity proved to be a difficult challenge. Metals are typically removed from porphyrinoid cavities by treatment with acid; however, treatment with many different acids failed to produce any metal-free Cz. Similar difficulties were encountered in attempts to prepare metal-free TBC.¹³ To overcome this critical roadblock, we developed the reductive demetalation strategy shown in Figure 2. Treatment of $[(\text{TBP}_8\text{Cz})\text{P}^{\text{V}}(\text{OH})]\text{OH}$ with Na/NH_3 at -78°C followed by protonation gives the key, metal-free compound TBP_8CzH_3 . With this compound in hand, the door was open to transition metal corrolazine chemistry.

Reversible Oxygen Binding

The cobalt(III) complex $(\text{TBP}_8\text{Cz})\text{Co}^{\text{III}}$ was easily synthesized from TBP_8CzH_3 , and in the presence of strong axial ligands, five- and six-coordinate complexes $[(\text{TBP}_8\text{Cz})\text{Co}^{\text{III}}(\text{PPh}_3)]$ and $(\text{TBP}_8\text{Cz})\text{Co}^{\text{III}}(\text{pyr})_2$ were structurally characterized. From these structures, it was found that the metal-binding cavity of the Cz ligand is significantly smaller than porphyrins or even the conventional corroles. Despite the small central core, it was clear that the Cz ligand was competent to bind transition metal ions either out of plane as seen for $[(\text{TBP}_8\text{Cz})\text{Co}^{\text{III}}(\text{PPh}_3)]$ or completely in plane as seen for $[(\text{TBP}_8\text{Cz})\text{Co}^{\text{III}}(\text{pyr})_2]$.¹⁴

Although cobalt(II) porphyrins are well known to reversibly bind O_2 ,¹⁵ reports of cobalt corroles exhibiting reversible O_2 binding were curiously absent. It was suggested that cobalt(II) corroles were incapable of binding O_2 on the basis of electronic arguments.¹⁶ Reduction of $(\text{TBP}_8\text{Cz})\text{Co}^{\text{III}}$ by NaBH_4 in pyridine gives

$[(\text{TBP}_8\text{Cz})\text{Co}^{\text{II}}(\text{py})]^-$. This complex reversibly binds O_2 at low temperatures as monitored by EPR spectroscopy (Figure 3).¹⁷ The Co^{III} -superoxo complex is favored at temperatures of $\leq 240\text{ K}$. Reversible O_2 binding is observed for our complex but not for the conventional corroles most likely because a d_{z^2} ground state is present in $[(\text{TBP}_8\text{Cz})\text{Co}^{\text{III}}(\text{py})]^-$, which is a prerequisite for O_2 binding. For cobalt(II) corroles, the ground state appears to be different.^{16,18} These results were an early indication that the corrolazine platform could exhibit properties that were novel compared to those of the conventional corroles.

A Mn(V)-Oxo Complex

As in the case of cobalt, a manganese(III) corrolazine was easily prepared from TBP_8CzH_3 .^{19,20} The X-ray structure of this complex (Figure 4) reveals that a molecule of MeOH from the crystallization solvent is coordinated as an axial ligand. Spectroscopic evidence suggests that in the absence of MeOH the Mn is four-coordinate.²¹ Neutral (e.g., R_3PO) and anionic axial ligands (e.g., Cl^-) bind very tightly to this complex [$K_a(\text{Cl}^-) = 1.3(4) \times 10^7\text{ M}^{-1}$], consistent with the starting material being four-coordinate. The five-coordinate chloride complex has been structurally characterized (vide infra).

The first high-valent metalcorrolazine of relevance to oxygen-derived porphyrinoid species was obtained with the synthesis of a manganese(V)-oxo complex, $(\text{TBP}_8\text{Cz})\text{Mn}^{\text{V}}(\text{O})$.^{19,20} The two-electron oxidation of $(\text{TBP}_8\text{Cz})\text{Mn}^{\text{III}}$ by mCPBA or PhIO takes place with O atom transfer to give the high-valent metal-oxo species, $(\text{TBP}_8\text{Cz})\text{Mn}^{\text{V}}(\text{O})$ (Figure 4). This complex exhibits a remarkable stability; it is isolable at room temperature and can be purified without special precautions by standard silica gel chromatography. Only one other type of ligand

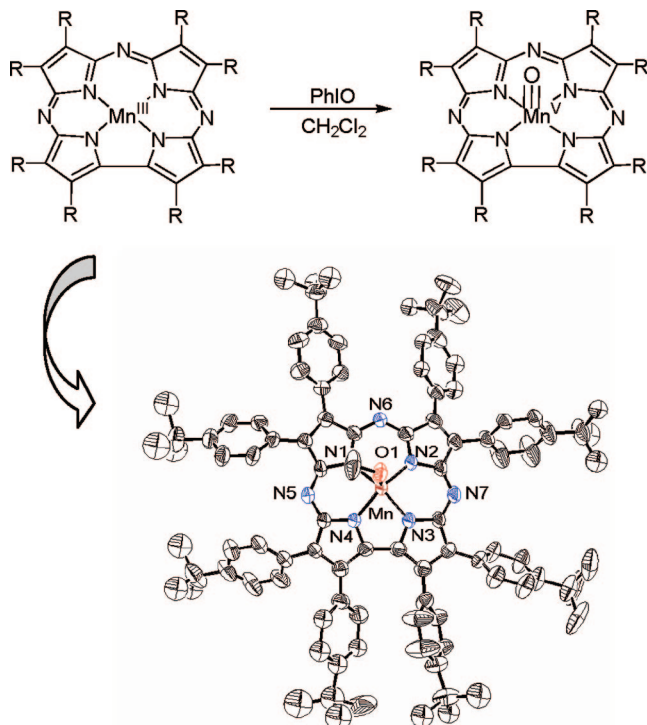


FIGURE 4. Synthesis of $(\text{TBP}_8\text{Cz})\text{Mn}^{\text{V}}(\text{O})$ and X-ray structure of $(\text{TBP}_8\text{Cz})\text{Mn}^{\text{III}}(\text{HOMe})$.

is able to stabilize a $\text{Mn}^{\text{V}}\text{-oxo}$ complex for isolation,^{22,23} and a $\text{Mn}^{\text{V}}\text{-oxo}$ porphyrin has been described that is stable for ~ 1 min at room temperature.^{24,25} Corrole $\text{Mn}^{\text{V}}\text{-oxo}$ complexes have also been reported but exhibit limited stability in solution.^{26,27}

Characterization of $(\text{TBP}_8\text{Cz})\text{Mn}^{\text{V}}(\text{O})$ was carried out by MALDI-MS, NMR, resonance Raman, and XANES/EXAFS.^{19,20} The NMR spectrum is diamagnetic, which indicates a low-spin Mn^{V} (d^2) complex. The triply bonded terminal oxo ligand gives rise to a peak in the RR spectrum at 979 cm^{-1} in CH_2Cl_2 , which shifts as predicted for a simple diatomic oscillator to 938 cm^{-1} after facile exchange with H_2^{18}O . Although crystals of sufficient quality for XRD have eluded us, structural information was obtained through XANES/EXAFS data and revealed a short Mn–O bond of $1.56(2)\text{ \AA}$. There is also an intense XANES pre-edge feature (Figure 5) that is characteristic of $\text{M}=\text{E}$ species with $d^0\text{-}d^2$ electron counts ($\text{M} = \text{Mn, Ti, V, or Cr}$; $\text{E} = \text{O or N}$). Taken together, these data provided a definitive characterization for the structure and oxidation state of $(\text{TBP}_8\text{Cz})\text{Mn}^{\text{V}}(\text{O})$. Thus, this complex is a rare example of a stable, well-characterized $\text{Mn}^{\text{V}}\text{-oxo}$ complex, and its spectroscopic signatures provide important benchmark information for the identification of $\text{Mn}^{\text{V}}\text{-oxo}$ species proposed as intermediates in biological systems and catalytic reactions.²⁸

Spectroelectrochemical measurements of $(\text{TBP}_8\text{Cz})\text{-Mn}^{\text{III}}$ and $(\text{TBP}_8\text{Cz})\text{Mn}^{\text{V}}(\text{O})$ showed that the Mn^{III} complex can be electrochemically oxidized to the $\text{Mn}^{\text{V}}\text{-oxo}$ complex in pyridine with H_2O as the presumed O atom source.¹⁹ This result suggests that outer-sphere oxidants may be used in combination with H_2O to prepare high-valent metal–oxo corrolazines, but this idea has not yet

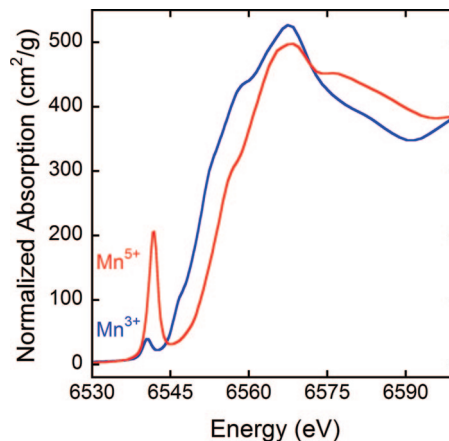


FIGURE 5. XANES spectra for $(\text{TBP}_8\text{Cz})\text{Mn}^{\text{V}}(\text{O})$ (red) and $(\text{TBP}_8\text{Cz})\text{Mn}^{\text{III}}$ (blue).

been tested. Electrochemical or chemical (Cp_2Co) reduction of the $\text{Mn}^{\text{V}}\text{-oxo}$ complex does not give a $\text{Mn}^{\text{IV}}\text{-oxo}$ complex but rather leads to production of $(\text{TBP}_8\text{Cz})\text{Mn}^{\text{III}}$, or a $\text{Mn}^{\text{III}}\text{-O-Mn}^{\text{IV}}$ species as seen by EPR spectroscopy. The terminal $\text{Mn}^{\text{IV}}\text{-oxo}$ complex is apparently unstable and has thus far eluded characterization. Cyclic voltammetric measurements reveal a reversible $\text{Mn}^{\text{V}}/\text{Mn}^{\text{IV}}$ couple at -0.05 V versus the SCE, which indicates that the $\text{Mn}^{\text{V}}\text{-oxo}$ complex is a rather mild oxidant for such a high-valent species. However, $(\text{TBP}_8\text{Cz})\text{Mn}^{\text{V}}(\text{O})$ was in fact found capable of selective oxidation chemistry, as described below.

Oxygen Atom Transfer (OAT) Reactions

Initial experiments established that rapid and quantitative OAT takes place between $(\text{Cz})\text{Mn}^{\text{V}}(\text{O})$ and PPh_3 to give OPPh_3 and $(\text{Cz})\text{Mn}^{\text{III}}$.²⁹ Isotopic labeling of the terminal oxo ligand with ^{18}O (via exchange with H_2^{18}O) provided a probe for the mechanism of this reaction. Significant incorporation of ^{18}O was found in the OPPh_3 product by gas chromatography–mass spectrometry (GC–MS), indicating a direct OAT mechanism. The $\text{Mn}^{\text{V}}\text{-oxo}$ complex was also competent to oxidize PhSMe to $\text{PhS}(\text{O})\text{Me}$, but only 45% conversion was observed after 24 h at room temperature. This reaction was significantly slower than with PPh_3 as the substrate, but sulfoxidation was still a thermodynamically favorable process.³⁰ No reaction between $(\text{Cz})\text{Mn}^{\text{V}}(\text{O})$ and *cis*-stilbene took place after 48 h at room temperature, suggesting that the $\text{Mn}^{\text{V}}\text{-oxo}$ complex was not thermodynamically competent for epoxidation of this substrate. With alkenes, we had seemingly reached the limit of OAT reactivity for $(\text{Cz})\text{Mn}^{\text{V}}(\text{O})$.

Interestingly, a dramatic enhancement in the apparent reactivity of $(\text{Cz})\text{Mn}^{\text{V}}(\text{O})$ was observed under catalytic conditions. We examined the sulfoxidation reaction where the Mn^{III} complex was added as a catalyst and PhIO was added as the external oxidant (Figure 6). These conditions yielded 86% sulfoxide in only 5 h at room temperature, equivalent to 165 turnovers. This rapid rate appeared inconsistent with the results from the stoichiometric reaction of $(\text{Cz})\text{Mn}^{\text{V}}(\text{O})$ with the same substrate. Even more surprisingly, the catalytic oxidation of *cis*-stilbene

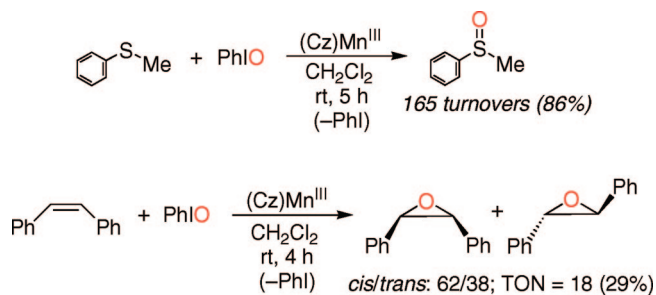


FIGURE 6. Catalytic sulfoxidation (top) and catalytic epoxidation (bottom) with a Mn^{III} corrolazine as catalyst and PhIO as an added oxidant.

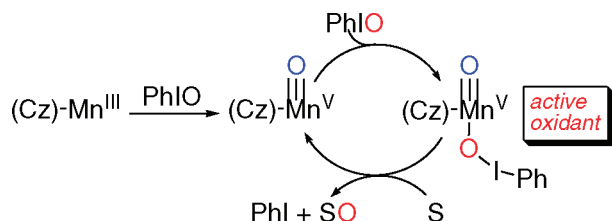


FIGURE 7. Proposed mechanism for OAT reactions catalyzed by manganese corrolazine with PhIO as an added oxidant.

led to the production of 29% epoxide in 4 h, with a significant preference for *cis*- over *trans*-epoxide product. This result was in clear conflict with the complete lack of reactivity between isolated (Cz)Mn^V(O) and *cis*-stilbene. It seemed impossible that (Cz)Mn^V(O) could be the active oxidant in these catalytic transformations, and we were inspired to postulate mechanistic alternatives that did not rely on direct OAT between (Cz)Mn^V(O) and substrate.

A proposed mechanism that brings together the experimental observations is shown in Figure 7. The initial formation of (Cz)Mn^V(O) is followed by a second equivalent of PhIO adding *trans* to the terminal oxo ligand. This coordinated PhIO adduct functions as the active oxidant, and it is the *coordinated O atom from PhIO, not the terminal oxo ligand*, that is transferred to substrate. The Mn^V-oxo species is serving as a Lewis acid to activate PhIO toward OAT. There is precedent for metal-bound PhIO complexes with both porphyrin and non-porphyrin (e.g., salen) coligands.^{31–34} Additional confirmation of the mechanism in Figure 7 was obtained through ¹⁸O labeling experiments, where it was shown that the terminal O atom *does not transfer* to substrate but the O atom in the bound PhIO does become incorporated into the oxidized product.

The proposed active oxidant in Figure 7 is formally a combination of the two species critical to heme enzyme and porphyrin-catalyzed oxidations (Figure 8, **A** and **B**). Species **B** is usually invoked as the active oxidant,^{1,2} but some evidence suggests **A** (the so-called “second oxidant” for cytochrome P450) is responsible for substrate oxidation in certain cases.^{35,36} Interestingly, much of the product distribution data for porphyrin-catalyzed reactions can be rationalized by invoking the active oxidant in Figure 7. Thus, this type of species could play a role in certain porphyrin-catalyzed oxidations. The proposed mechanism in Figure 7 may also explain observations regarding PhIO epoxidations catalyzed by Mn corroles, where again the

active catalytic species is not the expected Mn^V-oxo complex.^{26,27} We were excited to learn that the importance of the mechanism in Figure 7 has been underscored by recent work from Abu-Omar and co-workers, who provide compelling evidence that an analogous mechanism applies to the related NR group transfer in manganese corrole-catalyzed aziridinations.³⁷ Through elegant double-labeling and kinetic experiments, the active oxidant is shown to be most likely [(tpfc)Mn^V(NTs^{tBu})(ArINTs)], a Mn^V terminal imido complex with the catalytically active NR group coordinated *trans* to the imido ligand. It will be of interest to see if the active oxidant shown in Figure 7 becomes more prevalent in future mechanistic proposals for porphyrin, and especially corrole-catalyzed, oxidation chemistry.

Hydrogen Atom Abstraction Reactions

In parallel with OAT reactions, the process of hydrogen atom abstraction by high-valent metal-oxo porphyrinoid compounds is of widespread importance for proposed mechanisms of heme enzymes (e.g., cytochrome P450) and numerous synthetic porphyrin-catalyzed oxidations.² We knew from electrochemical measurements that the reduction potential of (Cz)Mn^V(O) (−0.05 V vs the SCE) was relatively low, suggesting that this complex would at best have a weak affinity for a H atom, given that the thermodynamics of H atom abstraction can be divided into the affinity for an electron and proton.³⁸ We were surprised to discover that in fact (Cz)Mn^V(O) reacted rapidly with a series of substituted phenols introduced as H-atom donors.³⁹ The phenol 2,4,6-*t*-Bu₃C₆H₂OH yields a stable phenoxyl radical that can easily be detected by EPR spectroscopy and was thus selected as a first test case. The oxidation of this substrate by (Cz)Mn^V(O) rapidly produced the radical as seen by EPR. However, there was no evidence for the generation of (Cz)Mn^{IV}(OH), which would be the logical product from a reaction between (Cz)Mn^V(O) and the phenol. Instead, isobestic conversion of the Mn^V complex to (Cz)Mn^{III} as monitored by UV-vis spectroscopy was observed upon addition of excess phenol. These data suggested that the putative (Cz)Mn^{IV}(OH) species does not accumulate. Quantitative confirmation of net H-atom abstraction was obtained by employing 2,4-*t*-Bu₂C₆H₂OH, which produced the expected *ortho*-linked bis(phenol) dimer in 80% yield.

Mechanistic insights into these reactions were obtained by kinetic analysis of a series of *para*-substituted phenols (4-X-2,6-*t*-Bu₂C₆H₂OH, where X = H, Me, OMe, or CN). The kinetics indicated a second-order rate law, and a Hammett plot with a ρ of −1.26 was obtained, consistent with concerted H-atom abstraction as the rate-determining step.⁴⁰ A linear correlation of log *k*' with BDE(O-H) was found and provided a second indication of a rate-limiting H-atom abstraction mechanism.³⁸ This mechanism (step I, Figure 9) was also strongly supported by the observation of a significant kinetic isotope effect (*k*_H/*k*_D) of 5.9 (ArO-H vs ArO-D) and a dramatic decrease in rate upon steric congestion (nearly 40 times faster for 2,4-*t*-

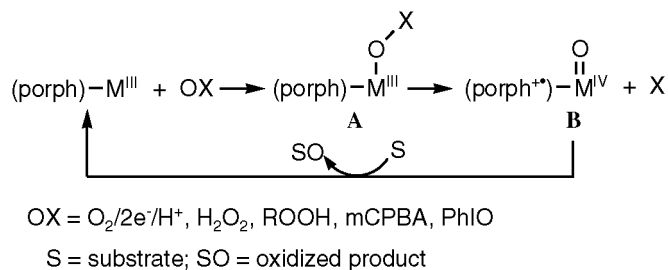


FIGURE 8. Simplified mechanism of porphyrin-catalyzed OAT reactions.

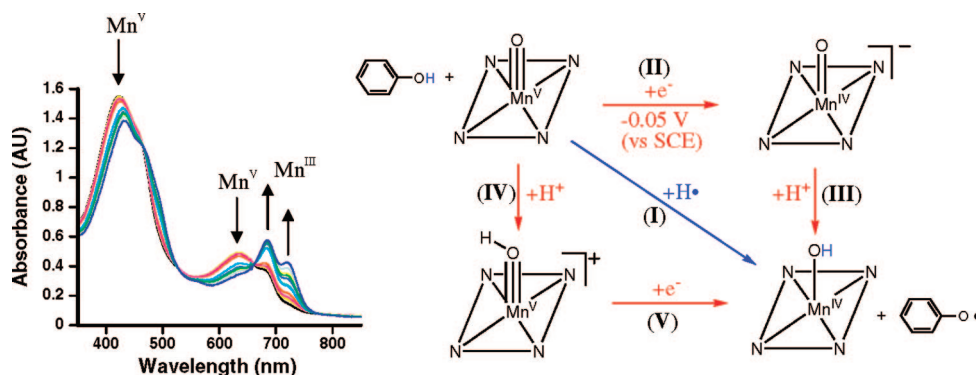


FIGURE 9. Oxidation of 2,4,6-*t*-Bu₃C₆H₂OH by [(TBP₈Cz)Mn^V(O)] as monitored by UV-vis spectroscopy and possible mechanistic pathways for the initial H-atom abstraction step.

Bu₂C₆H₃OH than for 2,4,6-*t*-Bu₃C₆H₂OH). Other possible pathways, such as electron transfer (ET/PT, steps II and III), or the opposite pathway (PT/ET, steps IV and V), were determined not viable on the basis of a combination of kinetic and electrochemical data. Hydrogen atom abstraction also occurred with C-H bonds similar in strength to the O-H bonds in phenols (e.g., dihydroanthracene), albeit at much slower rates.³⁹

The thermodynamics of the H-atom abstraction step (I) can be assessed on the basis of the component ET/PT pathways. Assuming that the O-H bond formed in the putative (Cz)Mn^{IV}(OH) species needs to be similar to or stronger than the O-H bond broken in the phenols [BDE(ArO-H) ~ 80 kcal/mol] for a thermodynamically favored process, a lower limit for BDE(MnO-H) of ~80 kcal/mol can be estimated. The BDE for the Mn complex is then related to the thermodynamic quantities in eq 1:

$$\text{BDE} = 23.06E^{1/2} + 1.37\text{p}K_{\text{a}} + C \quad (1)$$

where $E^{1/2}$ comes from step II, the $\text{p}K_{\text{a}}$ comes from step III, and C is a constant.³⁸ Thus, if a value of 80 kcal/mol is estimated for the BDE of (Cz)Mn^{IV}(OH) and $E^{1/2}(\text{Mn}^{\text{V}}/\text{Mn}^{\text{IV}}) = -0.05 \text{ V}$,¹⁹ eq 1 predicts a $\text{p}K_{\text{a}}$ of 22 for (Cz)-Mn^{IV}(OH). Even if a value as low as 70 kcal/mol is assumed for the (Cz)Mn(OH) bond strength, a $\text{p}K_{\text{a}}$ of 15 is predicted, indicating that the deprotonated [(Cz)Mn^{IV}(O)]⁻ is highly basic. This “back-of-the-envelope” calculation provides an explanation for the somewhat surprising reactivity of (Cz)Mn^V(O) toward H-atom abstraction. Significant driving force for H-atom abstraction comes from the affinity for the proton (i.e., the basicity) of the incipient [(Cz)Mn^{IV}(O)]⁻ species. It is

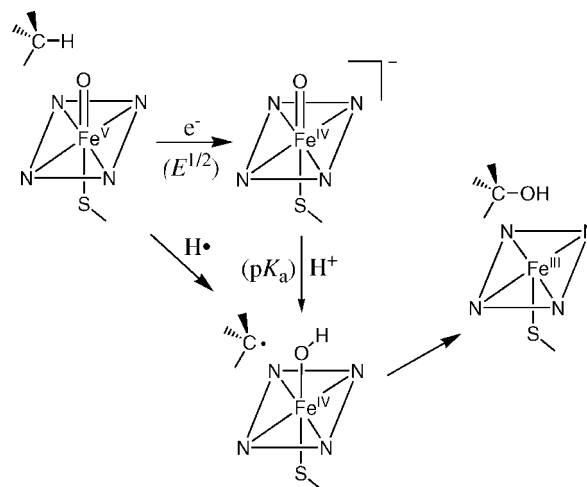


FIGURE 10. Hydrogen atom abstraction mechanism for cytochrome P450 showing the component ET and PT steps.

unusual to think of a high-valent metal-oxo species as a strong base, but in this case, the overall anionic charge of this complex makes this concept more reasonable.

Interestingly, these results fall in line nicely with recent ideas regarding the mechanism of cytochrome P450 (Figure 10). Mössbauer data and DFT calculations on P450 from Green and co-workers suggest that the ferryl intermediate (Cpd II) is protonated, giving a metal-hydroxo complex [(porph)(RS)Fe^{IV}(OH)], in agreement with their earlier results on the related thiolate-ligated heme enzyme chloroperoxidase (CPO).^{41,42} Protonation of P450-II and CPO-II implies that the Fe^{IV}-oxo unit is basic, and this enhanced basicity may arise from the additional negative charge provided by the proximal thiolate ligation found in P450 and CPO. Thus, Cpd I is reactive enough to oxidize

inert C–H bonds without accessing an exceedingly high redox potential. This concept provides a possible explanation for the long-standing question of how such a powerful oxidant can occur in a protein without destroying the protein itself through indiscriminate oxidation. To our knowledge, the reactivity of $(\text{TBP}_8\text{Cz})\text{Mn}^{\text{V}}(\text{O})$, which is at the same redox level as Cpd I, provides the first demonstration of this concept in a well-characterized metalloporphyrinoid complex. There is also a satisfying parallel between the proposed role of the negatively charged thiolate ligand in Cpd II and the extra negative charge provided by the corrolazine ligand.

Mn(V)–Imido Corrolazine

The nitrogen-based, isoelectronic analogue of $(\text{TBP}_8\text{Cz})\text{Mn}^{\text{V}}(\text{O})$ is a terminal imido complex, $(\text{Cz})\text{Mn}^{\text{V}}(\text{NR})$, where the NR donor carries a formal charge of -2 . Terminal imido complexes have been postulated as the active intermediates in synthetically important NR group transfer reactions but have proven to be elusive with respect to direct characterization.^{43–45} Initial attempts to prepare $(\text{TBP}_8\text{Cz})\text{Mn}^{\text{V}}(\text{NR})$ relied on the thermal activation of alkyl or benzyl azides in the presence of $(\text{TBP}_8\text{Cz})\text{Mn}^{\text{III}}$, but these methods failed to give the desired product. During the course of our studies, Abu-Omar and co-workers discovered that the thermal or photolytic activation of aryl azides in the presence of Mn(III) corrole led to the synthesis of $(\text{corrole})\text{Mn}^{\text{V}}(\text{NAr})$, the first example of a well-characterized Mn(V)–imido complex.⁴⁶

Following this method, we successfully prepared the high-valent imido complex $(\text{TBP}_8\text{Cz})\text{Mn}^{\text{V}}(\text{NMe})$ (Mes = mesityl).⁴⁷ As found for the oxo analogue, this complex was easily purified by standard bench-top chromatography and definitively characterized by XRD (Figure 11). The crystal structure revealed a short Mn–N_{imido} bond distance [1.595(4) and 1.611(4) Å for two independent molecules] and a linear Mn–N_{imido}–C angle [179.7(4)° and 176.9(4)°], characteristic of a Mn–N triple bond. Comparison with a Mn–N_{imido} bond distance of 1.613(4) Å and a Mn–N_{imido}–C angle of 170.4(4)° for $(\text{tpfc})\text{Mn}^{\text{V}}(\text{NMe})$ suggests there is slightly better π -overlap between the imido ligand and the d_{xz}/d_{yz} orbitals of the manganese in the corrolazine.

Analysis of $(\text{TBP}_8\text{Cz})\text{Mn}^{\text{V}}(\text{NMe})$ by ¹H NMR showed a diamagnetic spectrum, indicative of an authentic low-spin Mn^V complex. Interestingly, the peaks for the aryl protons of the Cz ligand are not separated on the basis of their relation to the NMe axial ligand, indicating that free rotation occurs about the C_{pyrrole}–C_{aryl} bonds despite the apparent steric crowding of the eight *para-tert*-butylphenyl substituents. A similar ¹H NMR spectrum is seen for $(\text{TBP}_8\text{Cz})\text{Mn}^{\text{V}}(\text{O})$, where the aryl proton resonances are equivalent with respect to the terminal oxo group.

The Mn^V–imido complex proved to be remarkably inert to reduction. Addition of alkenes to the imido complex did not yield aziridine products, even under forcing conditions (e.g., prolonged heating with excess cyclooctene). The Mn(V)–oxo complex was also inert to the analogous epoxidation of alkenes, so this result was

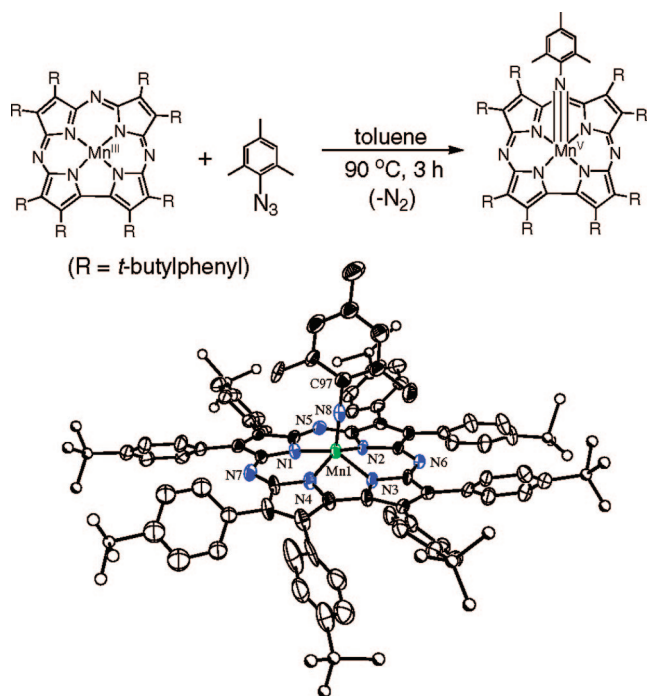


FIGURE 11. Synthesis and X-ray structure of $(\text{TBP}_8\text{Cz})\text{Mn}^{\text{V}}(\text{NMe})$.

perhaps not totally unexpected. However, the imido complex was also unreactive toward hydrogen atom transfer agents such as phenols or even TEMPO-H, which has a very weak O–H bond (BDE = 70 kcal/mol), in contrast to the Mn^V–oxo complex. Cyclic voltammetric measurements provided an important clue regarding this apparent lack of reactivity. The first reduction wave for $(\text{TBP}_8\text{Cz})\text{Mn}^{\text{V}}(\text{NMe})$ does not appear until -1.36 V versus Ag/AgCl and is assigned to a Cz ring reduction. There is no evidence of a metal reduction process. Confirmation of the inertness of $(\text{Cz})\text{Mn}^{\text{V}}(\text{NMe})$ came from a lack of reactivity with an excess of the strong one-electron reductant Cp₂Co ($E^{1/2} = -0.95$ V). The lack of reactivity with H-atom transfer agents was now more understandable, since part of the thermodynamic driving force for H-atom abstraction comes from the favorability of the putative Mn^{V/IV} couple (eq 1), which is totally absent for $(\text{TBP}_8\text{Cz})\text{Mn}^{\text{V}}(\text{NMe})$.

Interestingly, the corrole analogue $(\text{tpfc})\text{Mn}^{\text{V}}(\text{NAr})$ is relatively easy to reduce ($E^{1/2} = -0.36$ V vs Ag/AgCl).⁴⁸ Typically, substitution of the more electronegative nitrogen atoms for carbon atoms at the *meso* positions on going from corrolazine to corrole makes the molecule *more difficult* to reduce,¹⁰ but the opposite trend is seen here. It is possible that the π -donation from the imido ligand to Mn^V in $(\text{TBP}_8\text{Cz})\text{Mn}^{\text{V}}(\text{NMe})$ is better than that in the corrole complex, as suggested by the structural parameters. This effect may compensate for the electron-poor nature of the *meso*-N-substituted ring system, making it more difficult to reduce the corrolazine complex.

The first reversible oxidation wave ($E^{1/2} = 0.71$ V) for $(\text{TBP}_8\text{Cz})\text{Mn}^{\text{V}}(\text{NMe})$ is shifted to a lower potential compared to the first oxidation for $(\text{TBP}_8\text{Cz})\text{Mn}^{\text{V}}(\text{O})$ (1.02 V)¹⁹ or $(\text{tpfc})\text{Mn}^{\text{V}}(\text{NMe})$ (1.21 V).⁴⁸ Chemical oxidation of

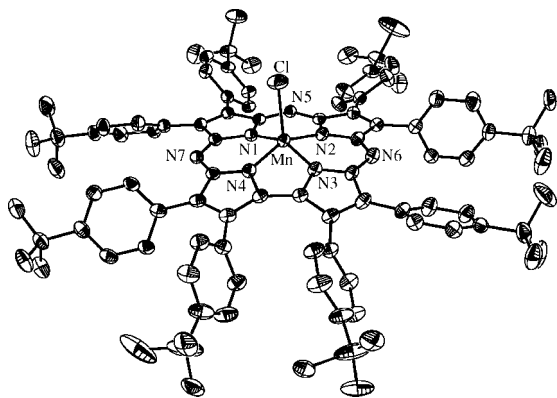


FIGURE 12. ORTEP diagram of $[(\text{TBP}_8\text{Cz})\text{Mn}(\text{Cl})]^-$ showing 50% probability thermal ellipsoids. Hydrogen atoms have been removed for the purpose of clarity.

$(\text{TBP}_8\text{Cz})\text{Mn}^{\text{V}}(\text{NMe}_2)$ with $[(4\text{-BrC}_6\text{H}_4)_3\text{N}]^+\text{SbCl}_6^-$ led to a new species characterized as a π -cation–radical complex, $[(\text{TBP}_8\text{Cz}^+)\text{Mn}^{\text{V}}(\text{NMe}_2)]^+$, which appeared to be stable in solution and could be quantitatively reduced back to the neutral Mn^{V} complex using Cp_2Co . A Mn^{VI} complex does not appear to form in this case, as opposed to the oxidation of the related nitrido corrole species $[(\text{corrole})\text{Mn}^{\text{V}}=\text{N}]^-$, which has been reported to give a Mn^{VI} species as seen by EPR spectroscopy.⁴⁹ These results emphasize that the potential “innocence” of the corrole/corrolazine ligand needs to be evaluated on a case-by-case basis.

O–O Bond Cleavage of Hydrogen Peroxide

Our success in isolating the Mn^{V} -oxo and Mn^{V} -imido complexes demonstrated that the TBP_8Cz platform was capable of stabilizing high-valent species which are normally fleeting intermediates with conventional porphyrin ligands. Thus, we believed the corrolazine system would be useful for testing mechanistic concepts regarding O–O bond cleavage from dioxygen-derived oxidants (e.g., H_2O_2), since the expected high-valent product should be directly observable. Addition of H_2O_2 to $(\text{Cz})\text{Mn}^{\text{III}}$ does not give $(\text{Cz})\text{Mn}^{\text{V}}(\text{O})$. However, we discovered a dramatic axial ligand effect for this reaction, where the $(\text{Cz})\text{Mn}^{\text{III}}$ complex does react with H_2O_2 after coordination by an anionic axial ligand.

Addition of Et_4NCl to $(\text{TBP}_8\text{Cz})\text{Mn}^{\text{III}}$ gives $\text{Et}_4\text{N}^+[(\text{TBP}_8\text{Cz})\text{Mn}^{\text{III}}(\text{Cl})]^-$, which was characterized by XRD (Figure 12).⁵⁰ This complex is the first example to our knowledge of a structurally characterized anionic corrole complex and demonstrates the corrolazine’s versatility in stabilizing both high-valent complexes and relatively low-valent, electron-rich species. Binding studies revealed that the Cl^- ligand is tightly coordinated in solution.¹⁹ Formation of the chloride complex in situ by addition of 1.1 equiv of Et_4NCl to $(\text{TBP}_8\text{Cz})\text{Mn}^{\text{III}}$ in CH_2Cl_2 , followed by treatment with excess H_2O_2 (30% aqueous), led to the rapid formation of the Mn^{V} -oxo complex as seen by UV–vis, and isolation by chromatography gave a yield of 63%. The proposed mechanism for this reaction (Figure

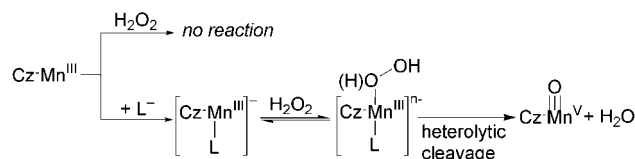


FIGURE 13. Activation of H_2O_2 with $(\text{Cz})\text{Mn}^{\text{III}}$ in the presence of anionic axial ligands to give $(\text{Cz})\text{Mn}^{\text{V}}(\text{O})$.

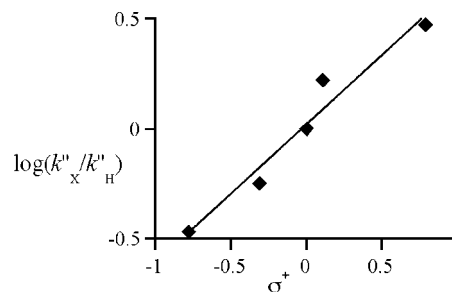


FIGURE 14. Hammett plot for the reaction of $[(\text{TBP}_8\text{Cz})\text{Mn}^{\text{III}}(\text{L})]^-$ with H_2O_2 ($\text{L}^- = p\text{-X-C}_6\text{H}_4\text{S}^-$), where the slope $= \rho = 0.63 \pm 0.08$. k_X'' is the observed second-order rate constant for the $p\text{-X}$ -substituted phenols except for k_{H}'' , where $\text{X} = \text{H}$.

13) involves coordination of H_2O_2 followed by heterolytic O–O bond cleavage and two-electron oxidation of the metal center. Homolytic cleavage is also possible but would lead to formation of a $\text{Mn}^{\text{IV}}\text{-O}(\text{H})$ complex that is likely unstable (*vide supra*) and not observed.

Addition of a series of *para*-substituted arylthiolate ligands ($p\text{-X-C}_6\text{H}_4\text{S}^-\text{Na}^+$, where $\text{X} = \text{H}, \text{OMe}, \text{CH}_3, \text{Cl},$ or NO_2) also induced the activation of H_2O_2 by the Mn^{III} complex. These anionic donors were chosen because they allowed for a comparison of electronic effects among a series of structurally similar axial ligands and because they would be good mimics for the thiolate donor found in P450, which has been postulated to provide an important electronic “push” effect in the enzyme’s critical O–O bond cleavage step. Smooth conversion of a Mn^{III} species to a Mn^{V} -oxo species was seen with these thiolate donors, and a kinetic analysis of these reactions gave a Hammett plot with a ρ of 0.63 ± 0.08 (Figure 14). The positive slope indicates that there is an *increase* in reaction rate with the *electron-withdrawing* nature of the arylthiolate donor. We were surprised by this trend, because it is the opposite of what would be expected for the normal push effect in metalloporphyrins, in which *electron-donating* axial ligands should increase the rate of O–O bond cleavage through either heterolytic or homolytic mechanisms.^{51,52} We therefore sought another way of confirming this inverse axial ligand effect. Cumene hydroperoxide is a useful probe for distinguishing between heterolytic and homolytic O–O bond cleavage,^{53,54} and a normal push effect should result in greater heterolytic cleavage with an increased level of donation of electron density from the axial ligand. As seen in Figure 15, the O–O bond cleavage is significantly influenced by the identity of the axial ligand, and that influence is the opposite of what is expected. The ratio of heterolytic to homolytic cleavage product clearly increases with the electron-withdrawing nature of the axial ligand for the *para*-substituted arylthiolate donors. It was also satisfying to find the same trend among a different type

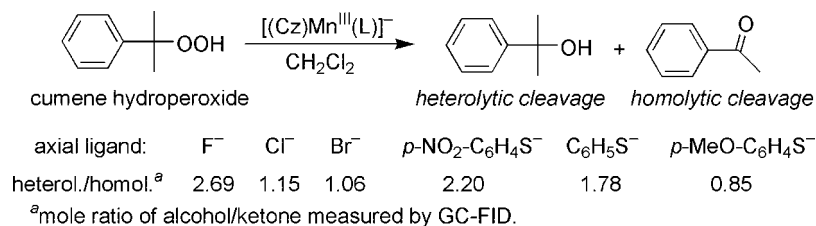


FIGURE 15. Trends in heterolytic vs homolytic O–O bond cleavage for cumene hydroperoxide and different axial ligands with (TBP₈Cz)Mn^{III}.

of donor atom with the series of halide ligands, where the ratio clearly increases with an increase in electronegativity ($F_{EN}^- = 4.2$, $Cl_{EN}^- = 2.8$, and $Br_{EN}^- = 2.7$). Thus, the inverted push effect appears to hold for both different peroxides (H_2O_2 vs $ROOH$) and different types of axial ligands (ArS^- and X^-). Recently, a similar inverse electron demand was observed for certain iron porphyrins and $H_2O_2/ROOH$.^{55–57} The origin of this effect for the Mn^{III} corrolazine remains to be determined.

Concluding Remarks

Metalloporphyrinoid compounds provide a rich molecular landscape for the study of biologically relevant mechanisms, the discovery of new catalysts, and the development of new materials and medicinal agents. We have synthesized a new porphyrinoid system that involves contraction of the tetrapyrrolic core, resulting in a smaller cavity and third negative charge. We are beginning to understand the unique properties imparted to the internal metal ion by this ligand, including its ability to stabilize high-valent states. The dramatic stability of a Mn^V-oxo corrolazine allows for its bench-top isolation but still does not prevent it from functioning in selective oxidations. This balance between the stability and reactivity of high-valent metalcorrolazines needs to be further exploited. The isolation, trapping, or spectroscopic identification of a Mn^{IV}-oxo complex would be an important advance, since this species appears to be significantly less stable and hence potentially a much better oxidant than the Mn^V-oxo complex. Since it has been shown that H_2O_2 can be activated with the right type of metalcorrolazine, an important goal to pursue is finding appropriate mid- to low-valent metal complexes that can react with the ultimate oxidant, O_2 , to give high-valent metal-oxo species.

Recently, an iron corrolazine, (TBP₈Cz)Fe^{III}, has been shown to catalyze the rapid and efficient oxidation of thioether substrates to sulfoxide with H_2O_2 as the oxidant, while in the absence of substrate, it efficiently catalyzes the disproportionation of H_2O_2 .⁵⁸ Further study of this iron corrolazine may lead to the identification of high-valent iron-oxo species of biological relevance and catalytic interest. We hope this work demonstrates that new metalloporphyrinoid species can be prepared and important mechanistic insights can be obtained via direct modification of the porphyrin nucleus and we hope it encourages others to continue the quest for novel porphyrinoid systems.

The National Science Foundation (Grants CHE0094095, CHE0606614, and CHE0089168), Johns Hopkins University, the Alfred P. Sloan Jr. Foundation, The American Chemical Society Petroleum Research Fund, and the Camille and Henry Dreyfus Foundation are acknowledged for their generous support. I am grateful to the many talented co-workers and collaborators listed in the references, without whom this work would not have been possible.

References

- (1) Meunier, B.; de Visser, S. P.; Shaik, S. Mechanism of oxidation reactions catalyzed by cytochrome P450 enzymes. *Chem. Rev.* **2004**, *104*, 3947–3980.
- (2) McLain, J. L.; Lee, J.; Groves, J. T. In *Biomimetic Oxidations Catalyzed by Transition Metal Complexes*; Meunier, B., Ed.; Imperial College Press: London, 2000; pp 91–169.
- (3) Licoccia, S.; Paolesse, R. Metal complexes with tetrapyrrole ligands III. *Struct. Bonding* **1995**, *84*, 71–133.
- (4) Van Caemelbecke, E.; Will, S.; Autret, M.; Adamian, V. A.; Lex, J.; Gisselbrecht, J.-P.; Gross, M.; Vogel, E.; Kadish, K. M. Electrochemical and spectral characterization of iron corroles in high and low oxidation states: First structural characterization of an iron(IV) tetrapyrrole π cation radical. *Inorg. Chem.* **1996**, *35*, 184–192.
- (5) Will, S.; Lex, J.; Vogel, E.; Adamian, V. A.; Van Caemelbecke, E.; Kadish, K. M. Synthesis, characterization, and electrochemistry of sigma-bonded cobalt corroles in high oxidation states. *Inorg. Chem.* **1996**, *35*, 5577–5583.
- (6) Vogel, E.; Will, S.; Tilling, A. S.; Neumann, L.; Lex, J.; Bill, E.; Trautwein, A. X.; Wieghardt, K. Metalcorroles with formally tetravalent iron. *Angew. Chem., Int. Ed.* **1994**, *33*, 731–735.
- (7) Ramdhanie, B.; Stern, C. L.; Goldberg, D. P. Synthesis of the first corrolazine: A new member of the porphyrinoid family. *J. Am. Chem. Soc.* **2001**, *123*, 9447–9448.
- (8) Gross, Z.; Gaili, N.; Saltsman, I. The first direct synthesis of corroles from pyrrole. *Angew. Chem., Int. Ed.* **1999**, *38*, 1427–1429.
- (9) Gryko, D. T.; Fox, J. P.; Goldberg, D. P. Recent advances in the chemistry of corroles and core-modified corroles. *J. Porphyrins Phthalocyanines* **2004**, *8*, 1091–1105.
- (10) Kerber, W. D.; Goldberg, D. P. High-valent transition metal corrolazines. *J. Inorg. Biochem.* **2006**, *100*, 838–857.
- (11) Fujiki, M.; Tabei, H.; Isa, K. New tetrapyrrolic macrocycle: α,β,γ -Triazatetrazabenzcorrole. *J. Am. Chem. Soc.* **1986**, *108*, 1532–1536.
- (12) Li, J.; Subramanian, L. R.; Hanack, M. Substituted α,β,γ -triazatetrazabenzcorrole: An unusual reduction product of a phthalocyanine. *Chem. Commun.* **1997**, 679–680.
- (13) Li, J.; Subramanian, L. R.; Hanack, M. Studies on phosphorus phthalocyanines and triazatetrazabenzcorroles. *Eur. J. Org. Chem.* **1998**, 2759–2767.
- (14) Ramdhanie, B.; Zakharov, L. N.; Rheingold, A. L.; Goldberg, D. P. Synthesis, structures and properties of a series of four-, five-, and six-coordinate cobalt(III) triazacorrole complexes: The first examples of transition metal corrolazines. *Inorg. Chem.* **2002**, *41*, 4105–4107.
- (15) Jones, R. D.; Summerville, D. A.; Basolo, F. Synthetic oxygen carriers related to biological systems. *Chem. Rev.* **1979**, *79*, 139–179.
- (16) Hush, N. S.; Woolsey, I. S. Optical and electron spin resonance spectra of cobalt complexes related to Vitamin B₁₂. *J. Chem. Soc., Dalton Trans.* **1974**, 24–34.
- (17) Ramdhanie, B.; Telser, J.; Caneschi, A.; Zakharov, L. N.; Rheingold, A. L.; Goldberg, D. P. An example of O_2 binding in a cobalt(II) corrole system and high-valent cobalt-cyano and cobalt-alkynyl complexes. *J. Am. Chem. Soc.* **2004**, *126*, 2515–2525.

- (18) Murakami, Y.; Matsuda, Y.; Sakata, K.; Yamada, S.; Tanaka, Y.; Aoyama, Y. Transition-metal complexes of pyrrole pigments. XVII. Preparation and spectroscopic properties of corrole complexes. *Bull. Chem. Soc. Jpn.* **1981**, *54*, 163–169.
- (19) Lansky, D. E.; Mandimutsira, B.; Ramdhanie, B.; Clausén, M.; Penner-Hahn, J.; Zvyagin, S. A.; Telsler, J.; Krzystek, J.; Zhan, R. Q.; Ou, Z. P.; Kadish, K. M.; Zakharov, L.; Rheingold, A. L.; Goldberg, D. P. Synthesis, characterization, and physicochemical properties of manganese(III) and manganese(V)-oxo corrolazines. *Inorg. Chem.* **2005**, *44*, 4485–4498.
- (20) Mandimutsira, B. S.; Ramdhanie, B.; Todd, R. C.; Wang, H. L.; Zareba, A. A.; Czernuszewicz, R. S.; Goldberg, D. P. A stable manganese(V)-oxo corrolazine complex. *J. Am. Chem. Soc.* **2002**, *124*, 15170–15171.
- (21) Licocchia, S.; Morgante, E.; Paolesse, R.; Polizio, F.; Senge, M. O.; Tondello, E.; Boschi, T. Tetracoordinated manganese(III) alkylcorrolates. Spectroscopic studies and the crystal and molecular structure of (7,13-dimethyl-2,3,8,12,17,18-hexaethylcorrolato)manganese(III). *Inorg. Chem.* **1997**, *36*, 1564–1570.
- (22) Collins, T. J.; Gordon-Wylie, S. W. A manganese(v)-oxo complex. *J. Am. Chem. Soc.* **1989**, *111*, 4511–4513.
- (23) Collins, T. J.; Powell, R. D.; Slobodnick, C.; Uffelman, E. S. A water-soluble manganese(V)-oxo complex: Definitive assignment of a $\nu_{\text{Mn=O}}$ infrared vibration. *J. Am. Chem. Soc.* **1990**, *112*, 899–901.
- (24) Jin, N.; Bourassa, J. L.; Tizio, S. C.; Groves, J. T. Rapid, reversible oxygen atom transfer between an oxomanganese(V) porphyrin and bromide: A haloperoxidase mimic with enzymatic rates. *Angew. Chem., Int. Ed.* **2000**, *39*, 3849–3851.
- (25) Jin, N.; Groves, J. T. Unusual kinetic stability of a ground-state singlet oxomanganese(V) porphyrin. Evidence for a spin state crossing effect. *J. Am. Chem. Soc.* **1999**, *121*, 2923–2924.
- (26) Gross, Z.; Golubkov, G.; Simkhovich, L. Epoxidation catalysts by a manganese corrole and isolation of an oxomanganese(V) corrole. *Angew. Chem., Int. Ed.* **2000**, *39*, 4045–4047.
- (27) Liu, H. Y.; Lai, T. S.; Yeung, L. L.; Chang, C. K. First synthesis of perfluorinated corrole and its Mn=O complex. *Org. Lett.* **2003**, *5*, 617–620.
- (28) Weng, T.-C.; Hsieh, W.-Y.; Uffelman, E. S.; Gordon-Wylie, S. W.; Collins, T. J.; Pecoraro, V. L.; Penner-Hahn, J. E. XANES evidence against manganyl species in the S_3 state of the oxygen-evolving complex. *J. Am. Chem. Soc.* **2004**, *126*, 8070–8071.
- (29) Wang, S. H. L.; Mandimutsira, B. S.; Todd, R.; Ramdhanie, B.; Fox, J. P.; Goldberg, D. P. Catalytic sulfoxidation and epoxidation with a Mn(III) triazacorrole: Evidence for a “third oxidant” in high-valent porphyrinoid oxidations. *J. Am. Chem. Soc.* **2004**, *126*, 18–19.
- (30) Holm, R. H.; Donahue, J. P. A thermodynamic scale for oxygen atom transfer reactions. *Polyhedron* **1993**, *12*, 571–589.
- (31) Smegal, J. A.; Schardt, B. C.; Hill, C. L. Isolation, purification, and characterization of intermediate (iodosylbenzene)metalloporphyrin complexes from the (tetraphenylporphinato)manganese(III)-iodosylbenzene catalytic hydrocarbon functionalization system. *J. Am. Chem. Soc.* **1983**, *105*, 3510–3515.
- (32) Adam, W.; Roschmann, K. J.; Saha-Moller, C. R.; Seebach, D. cis-Stilbene and (1 α ,2 β ,3 α)-(2-ethenyl-3-methoxycyclopropyl)benzene as mechanistic probes in the Mn^{III}. (salen)-catalyzed epoxidation: Influence of the oxygen source and the counterion on the diastereoselectivity of the competitive concerted and radical-type oxygen transfer. *J. Am. Chem. Soc.* **2002**, *124*, 5068–5073.
- (33) Nam, W.; Choi, S. K.; Lim, M. H.; Rohde, J. U.; Kim, I.; Kim, J.; Kim, C.; Que, L., Jr. Reversible formation of iodosylbenzene-iron porphyrin intermediates in the reaction of oxoiron(IV) porphyrin pi-cation radicals and iodobenzene. *Angew. Chem., Int. Ed.* **2003**, *42*, 109–111.
- (34) Nam, W. W.; Valentine, J. S. Reevaluation of the significance of O-18 incorporation in metal complex-catalyzed oxygenation reactions carried out in the presence of (H₂O)-O-18. *J. Am. Chem. Soc.* **1993**, *115*, 1772–1778.
- (35) Newcomb, M.; Hollenberg, P. F.; Coon, M. J. Multiple mechanisms and multiple oxidants in P450-catalyzed hydroxylations. *Arch. Biochem. Biophys.* **2003**, *409*, 72–79.
- (36) Ogliaro, F.; de Visser, S. P.; Cohen, S.; Sharma, P. K.; Shaik, S. Searching for the second oxidant in the catalytic cycle of cytochrome P450: A theoretical investigation of the iron(III)-hydroperoxo species and its epoxidation pathways. *J. Am. Chem. Soc.* **2002**, *124*, 2806–2817.
- (37) Zdilla, M. J.; Abu-Omar, M. M. Mechanism of catalytic aziridination with manganese corrole: The often postulated high-valent Mn(V) imido is not the group transfer reagent. *J. Am. Chem. Soc.* **2006**, *128*, 16971–16979.
- (38) Mayer, J. M. In *Biomimetic Oxidations Catalyzed by Transition Metal Complexes*; Meunier, B., Ed.; Imperial College Press: London, 2000; pp 1–43.
- (39) Lansky, D. E.; Goldberg, D. P. Hydrogen atom abstraction by a high-valent manganese(V)-oxo corrolazine. *Inorg. Chem.* **2006**, *45*, 5119–5125.
- (40) Pratt, D. A.; DiLabio, G. A.; Mulder, P.; Ingold, K. U. Bond strengths of toluenes, anilines, and phenols: To hammett or not. *Acc. Chem. Res.* **2004**, *37*, 334–40.
- (41) Behan, R. K.; Hoffart, L. M.; Stone, K. L.; Krebs, C.; Green, M. T. Evidence for basic ferryls in cytochromes P450. *J. Am. Chem. Soc.* **2006**, *128*, 11471–11474.
- (42) Stone, K. L.; Hoffart, L. M.; Behan, R. K.; Krebs, C.; Green, M. T. Evidence for two ferryl species in chloroperoxidase compound II. *J. Am. Chem. Soc.* **2006**, *128*, 6147–6153.
- (43) DuBois, J.; Tomooka, C. S.; Hong, J.; Carreira, E. M. Nitridomanganese(V) complexes: Design, preparation, and use as nitrogen atom-transfer reagents. *Acc. Chem. Res.* **1997**, *30*, 364–372.
- (44) Eikey, R. A.; Abu-Omar, M. M. Nitrido and imido transition metal complexes of Groups 6–8. *Coord. Chem. Rev.* **2003**, *243*, 83–124.
- (45) Mahy, J. P.; Bedi, G.; Battioni, P.; Mansuy, D. Aziridination of alkenes catalyzed by porphyrinirons: Selection of catalysts for optimal efficiency and stereospecificity. *J. Chem. Soc., Perkin Trans. 2* **1988**, 1517–1524.
- (46) Eikey, R. A.; Khan, S. I.; Abu-Omar, M. M. The elusive terminal imido of manganese(V). *Angew. Chem., Int. Ed.* **2002**, *41*, 3592–3595.
- (47) Lansky, D. E.; Kosack, J. R.; Sarjeant, A. A. N.; Goldberg, D. P. An isolable, non-reducible high-valent manganese(V) imido corrolazine complex. *Inorg. Chem.* **2006**, *45*, 8477–8479.
- (48) Edwards, N. Y.; Eikey, R. A.; Loring, M. I.; Abu-Omar, M. M. High-valent imido complexes of manganese and chromium corroles. *Inorg. Chem.* **2005**, *44*, 3700–3708.
- (49) Golubkov, G.; Gross, Z. Nitrogen atom transfer between manganese complexes of salen, porphyrin, and corrole and characterization of a (nitrido)manganese(VI) corrole. *J. Am. Chem. Soc.* **2005**, *127*, 3258–3259.
- (50) Lansky, D. E.; Sarjeant, A. A. N.; Goldberg, D. P. Inverse axial-ligand effects in the activation of H₂O₂ and ROOH by an Mn(III) corrolazine. *Angew. Chem., Int. Ed.* **2006**, *45*, 8214–8217.
- (51) Dawson, J. H. Probing structure-function relations in heme-containing oxygenases and peroxidases. *Science* **1988**, *240*, 433–439.
- (52) Ogliaro, F.; de Visser, S. P.; Shaik, S. The ‘push’ effect of the thiolate ligand in cytochrome P450: A theoretical gauging. *J. Inorg. Biochem.* **2002**, *91*, 554–567.
- (53) Ingold, K. U.; MacFaul, P. A. In *Biomimetic Oxidations Catalyzed by Transition Metal Complexes*; Meunier, B., Ed.; Imperial College Press: London, 2000; pp 45–89.
- (54) Watanabe, Y. In *The Porphyrin Handbook*; Kadish, K. M., Smith, K. M., Guilard, R., Eds.; Academic Press: New York, 2000; Vol. 4, pp 97.
- (55) Nam, W.; Han, H. J.; Oh, S. Y.; Lee, Y. J.; Choi, M. H.; Han, S. Y.; Kim, C.; Woo, S. K.; Shin, W. New insights into the mechanisms of O-O bond cleavage of hydrogen peroxide and tert-alkyl hydroperoxides by iron(III) porphyrin complexes. *J. Am. Chem. Soc.* **2000**, *122*, 8677–8684.
- (56) Nam, W.; Lim, M. H.; Oh, S. Y. Effect of anionic axial ligands on the formation of oxoiron(IV) porphyrin intermediates. *Inorg. Chem.* **2000**, *39*, 5572–5575.
- (57) Nam, W.; Lim, M. H.; Oh, S. Y.; Lee, J. H.; Lee, H. J.; Woo, S. K.; Kim, C.; Shin, W. Remarkable anionic axial ligand effects of iron(III) porphyrin complexes on the catalytic oxygenations of hydrocarbons by H₂O₂ and the formation of oxoiron(IV) porphyrin intermediates by m-chloroperoxybenzoic acid. *Angew. Chem., Int. Ed.* **2000**, *39*, 3646–3649.
- (58) Kerber, W. D.; Ramdhanie, B.; Goldberg, D. P. H₂O₂ oxidations catalyzed by an iron(III) corrolazine: Avoiding high-valent iron-oxido species? *Angew. Chem., Int. Ed.* **2007**, *46*, 3718–3721.

AR700039Y